Pretransitional fluctuations in the isotropic phase of a lyotropic chromonic liquid crystal

Yu. A. Nastishin,[1,2] H. Liu,[1] S. V. Shiyanovskii,[1] O. D. Lavrentovich,[1] A. F. Kostko,[3,4] and M. A. Anisimov[3,*]

[1]*Liquid Crystal Institute, Kent University, Kent, Ohio 44242, USA*
[2]*Institute for Physical Optics, 23 Dragomanov Str., Lviv, 79005 Ukraine*
[3]*Institute for Physical Science and Technology and Department of Chemical Engineering, University of Maryland, College Park, Maryland 20742, USA*
[4]*Department of Physics, St. Petersburg State University of Refrigeration and Food Engineering, St. Petersburg, 191002, Russia*

We have studied isotropic-to-nematic pretransitional fluctuations in an aqueous solution of disodium cromoglycate (cromolyn) by static and dynamic light scattering. Cromolyn is a representative of lyotropic chromonic liquid crystals with building units being elongated rods formed by aggregates of disk-like molecules. By combining light-scattering and viscosity measurements we have determined the correlation length and relaxation time of the orientational order-parameter fluctuations and estimated the size of the cromolyn aggregates. The pretransitional behavior of light scattering does not completely follow the classic Landau–de Gennes model. This feature is most probably associated with the variable length of cromolyn aggregates. We have observed a dramatic increase of the shear viscosity near the transition to the nematic phase, the fact which correlates with the idea of growing supramolecular aggregates. The steep temperature dependence of the viscosity is accompanied by a practically temperature-independent translational diffusion coefficient.

I. INTRODUCTION

Lyotropic chromonic liquid crystals (LCLCs) present an unusual example of lyotropic (solvent-dependent) mesomorphism [1–3]. The LCLC family embraces a range of materials known better as dyes, drugs and nucleic acids rather than as liquid crystals. The term chromonic, according to Lydon [1] who coined the term, is a short hand for phrases such as "lyotropic mesophase formed by soluble aromatic mesogens" that additionally was intended to carry connotations of dyes and chromosomes and of the bischromone structure of disodium cromoglycate (DSCG), one of the first solutes identified to form LCLCs [1,4]. DSCG is also known as cromolyn, Intal, and as disodium 5,5'-[(2-hydroxy-1,3-propanediyl)bis(oxy)]bis[4-oxy-4H-1-benzopyran-2-carboxylate] (the IUPAC nomenclature of the particular isomer used in this study). The LCLC molecules have a relatively rigid plank-like or disk-like aromatic core with polar solubilizing groups at the periphery. Aggregation of these molecules, caused by face-to-face arrangement of aromatic cores, results usually in cylindrical stacks with molecular planes in the case of DSCG being more or less perpendicular to the axis of the aggregate. The geometry of the basic structural unit in LCLCs is thus very different from micelles, spherical or cylindrical, and bilayers formed by amphiphilic (surfactant) molecules in the regular lyotropic liquid crystals [1–3,5]. The tendency to aggregate is observed even in very dilute solutions, so that, according to Lydon [1], the LCLCs do not seem to show a distinct threshold concentration similar to the critical micelle concentration in amphiphilic systems, except, perhaps, at the stage of dimer formation. In contrast to closed micelles, the LCLC aggregates do not have a clearly defined size (length), as there are no geometrical restrictions to adding another molecule to the existing stack. Such a behavior, first observed in studies of nucleic acid bases and nucleosides, is called "isodesmic" [1,2].

DSCG with a structural formula shown in Fig. 1 remains the most studied LCLC material [1,2,6,7]. One of the reasons is that DSCG is used as an effective antiasthmatic drug, although there is no clear link between its therapeutic activity and its mesomorphic properties. When dissolved in water, DSCG forms two mesomorphic phases, uniaxial nematic and columnar, labeled N and M, respectively [1,2,6–17]. The structural x-ray data [7] suggest that the DSCG molecules are arranged in cylindrical aggregates with their core regions being predominantly perpendicular to the axis of the cylinder. The intermolecular separation is about 0.34 nm along the aggregate axis. In the M phase, the aggregates are parallel to each other and arranged into a hexagonal lattice. In the N phase, formed at larger dilutions, this lattice is not present but the aggregates retain the orientational order, which makes the N phase similar to a regular nematic phase in
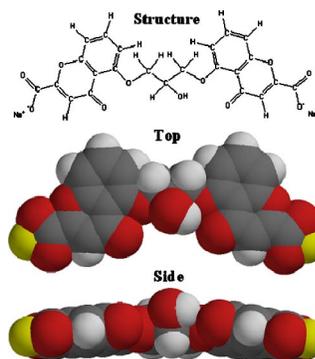

FIG. 1. (Color online) Structural formula and molecular model for DSCG.

*Corresponding author. Email address: anisimov@umd.edu

thermotropic (solvent-free) materials composed of elongated rod-like molecules. The scalar orientational order of DSCG aggregates is high, in the range 0.76–0.97, depending on the concentration [14].

The details of molecular packing within the DSCG aggregates are still being debated (see, for example, [15,16]). Originally, Hartshorne and Woodard [7] assumed that there is one molecule per circular cross section of the cylinder in DSCG aggregates. They estimated the cylinder diameter to be about 1.6 nm; this value is somewhat smaller than the extended length of the flat DSCG molecule (which is about 1.9 nm; see Fig. 1). Later, Lydon [8] proposed that the aggregate has a hollow square chimney shape formed by four molecules linked by electrostatic salt bridges. Hui and Labes argued [17] that the structure is similar to that of regular micelles. Namely, they claimed that there are four DSCG molecules in the cross section of the aggregate; these molecules have a shape of a sharp letter V with the OH group at the apex. The OH groups point towards the axis of the cylinder while the eight zwitterionic COONa groups point outward to the water continuum.

Despite the lack of complete understanding of supramolecular self-organization in LCLCs, it has recently become evident that some of these materials can be of practical use precisely because of their mesomorphic properties. Following the early works of Dryer [18], different research groups have explored the possibility of using dye-based LCLCs in the fabrication of polarizing [19–26] and optical compensating elements [27,28]. The main feature allowing such an application is that when water evaporates, the resulting dry film still preserves an orientational order and thus anisotropic optical properties. Preserved in-plane long-range orientational order has been demonstrated not only for films of micron thickness but also for nanofilms comprised of just one or a few stacked LCLC monolayers and fabricated by an electrostatic layer-by-layer deposition technique [29].

To expand the characterization of LCLCs and clarify the nature of the isotropic-nematic transition in such systems, we have performed dynamic and static light scattering on pretransitional fluctuations in the isotropic phase of the aqueous solution of DSCG. As compared to NMR and x-ray techniques used in the past to characterize the structural properties of LCLCs, the light scattering experiments enable one to gain an insight into the behavior of aggregates and mesoscopic fluctuations in the pre-transition region and to directly test the applicability of phenomenological models such as the Landau–de Gennes model. The concentration of DSCG was chosen to be 14 mass %, in order to study the phase transformation from the isotropic to the nematic state. Previously Champion and Meeten [6] have performed light-scattering experiments for much more dilute (about 1 mass %) samples. Their studies indicated that the two ring systems of DSCG are approximately coplanar; the configuration was though to be stabilized by multiple hydrogen bonds with the surrounding water molecules preserved even when the samples were dried [7].

By combining light-scattering and viscosity measurements we have been able to obtain the correlation length and relaxation time of the orientational order-parameter fluctuations and to deduce the dimensions of the DSCG aggregates.

The aggregates were found to grow up upon cooling the sample, causing a dramatic increase of the shear viscosity near the transition into the nematic phase. We also have found that the pretransitional behavior cannot be fully described by the classic Landau–de Gennes model; this fact can be explained by the temperature dependence of the length of the DSCG aggregates.

II. EXPERIMENT

A. Materials and sample preparation

The mixture studied in our light-scattering experiments, was a 14 mass % solution of DSCG in deionized water with an initial resistivity of 18 MΩ/cm. DSCG was obtained from the Spectrum Chemical Mfg. Corp. (Gardena, CA, CAS No. 15826-37-6). The measurements of the shear viscosity of the solution were performed with a rheometer DV-III, Brookfield.

The light-scattering measurements were performed at the University of Maryland, College Park. To avoid possible time dependence of the solution properties [6], the sample was heated prior to each experiment to $T=55$ °C, which is well above the temperature of disappearance of the nematic phase upon heating; then aged at 40 °C for 1 hour. The sample was kept at each experimental temperature for at least 20 minutes before measurements. The accuracy of temperature control was better than 0.01 °C. To check the absence of time dependence of the results, we repeated the experiment with the sample stored in an oven at 55 °C for three days. We found complete reproducibility of the light-scattering data and registered the same value $T_{NI}=31.8$ °C of the temperature, at which the first nematic nuclei appear on cooling.

B. Light-scattering-measurement procedure

A description of the experimental setup can be found in Ref. [30]. We measured the light-scattering intensity as well as the dynamic correlation function at each temperature T for a given scattering angle θ with two settings of the analyzer: VV and VH (where V and H denote the vertical and horizontal polarizations of light, respectively; the first symbol corresponds to the incident light and the second one to the scattered light). The optical arrangement is as follows: the scattering plane is horizontal while the polarization of the incident light is vertical, hence the measured intensity values I_{VV} and I_{VH} correspond to the settings VV and VH defined above. The measurements were conducted with ALV-5000/E and PhotoCor correlators for four different angles: 19°, 45°, 90° and 135° at various temperatures. Two groups of data were obtained: static and dynamic. Static (intensity) and dynamic (dynamic correlation function) data enabled us to obtain the information for the length scales and relaxation times of the inhomogeneities causing the light scattering.

At each temperature the light-scattering intensity, $I(t)$, was measured as a function of the time t every several seconds. The intensity values used in subsequent analysis were obtained from averaging $I(t)$ accumulated over time intervals of 10 minutes. Monitoring of $I(t)$ enables one to detect stray

light scattering from some submicron scatterers that may rarely appear in the scattering volume. This monitoring was useful in finding the temperature of the transition between isotropic-phase region and two-phase region where small drops of nematic phase appear. It helped us also to check that dust particles do not appear in the scattering volume. The intensity of the incident laser beam was also measured and its variations were accounted for corrections of light-scattering intensity data.

In the isotropic phase of a dust-free sample, light is scattered by fluctuations of the refractive index associated with fluctuations of different variables. In a solution of anisotropic molecules or anisotropic supramolecular aggregates the main contribution to the light-scattering intensity is associated with fluctuations of concentration and fluctuations of anisotropy [31]. Near the isotropic-nematic phase transition, the fluctuations of anisotropy are the fluctuations of the orientational order parameter [32,33], whereas the average value of the orientational order parameter is zero. The dynamics of these two types of fluctuations is different: concentration fluctuations (a conserved order parameter) relax to equilibrium by diffusion (the relaxation time depends on the length scale corresponding to the light-scattering wave number q), while fluctuations of anisotropy relax in first approximation independently of the length scale (nonconserved order parameter) [32–34]. The fluctuation modes can be independently identified from the static and dynamic light-scattering data. For the diffusive (isotropic) mode associated with isotropic fluctuations of concentration one can expect that $I_{\mathrm{VH}} = 0$ and thus the only contribution to the depolarized scattering will be from the anisotropic fluctuations. Therefore, a nonzero I_{VH} indicates the presence of orientational fluctuations that depolarize the scattered light. In addition to the orientational relaxation mode, in a solution of rod-shape scatterers, the depolarized component should contain a diffusion mode (dependent of q) associated with translational diffusion of rods [37,38]. However, close to the isotropic-nematic transition, the anisotropic fluctuation effects are dominant and, therefore, the mode associated with them should prevail. This mode eventually becomes critical, being accompanied by the critical slowing down, although the first-order phase transition occurs before the stability limit is reached.

III. PRETRANSITIONAL SUSCEPTIBILITY AND CORRELATION LENGTH

The vertically polarized component of the light-scattering intensity contains anisotropic and isotropic contributions:

$$I_{\mathrm{VV}} = (I_{\mathrm{VV}})_{\mathrm{an}} + I_{\mathrm{iso}}. \tag{1}$$

The depolarization ratio for fluctuations of anisotropy is given by [31,37,39]

$$\frac{I_{\mathrm{VH}}}{(I_{\mathrm{VV}})_{\mathrm{an}}} = \frac{3}{4}. \tag{2}$$

This is a rigorous result for fluctuations of the anisotropic part of the dielectric-permittivity tensor in the approximation
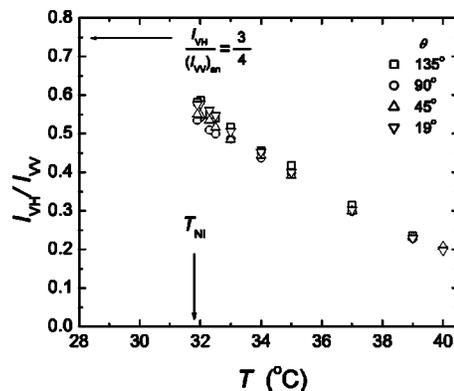

FIG. 2. Depolarization ratio of light scattered in the aqueous solution of DSCG (14 mass %) measured at four different scattering angles.

of a single correlation length. In practice, this ratio does never reach $\frac{3}{4}$ because of a contribution from the isotropic light scattering associated with fluctuations of density and concentration. Therefore, the isotropic part of the polarized light scattering can be extracted from the total intensity of the vertically polarized component as

$$I_{\mathrm{iso}} = I_{\mathrm{VV}} - \frac{4}{3} I_{\mathrm{VH}}. \tag{3}$$

The temperature behavior of the depolarization ratio $(I_{\mathrm{VH}}/I_{\mathrm{VV}})$ is shown in Fig. 2. The ratio increases upon approaching the temperature T_{NI}, at which the first nematic nuclei appear. However, $I_{\mathrm{VH}}/I_{\mathrm{VV}}$ does not reach the limiting value of 3/4 because of a significant contribution of isotropic scattering.

The anisotropic part of light scattering, $(I_{\mathrm{VV}})_{\mathrm{an}} = \frac{4}{3} I_{\mathrm{VH}}$, is caused by the fluctuations of the orientational order parameter and can be deduced from the standard Landau–de Gennes model of the isotropic-to-nematic phase transition as [32,39]

$$I_{\mathrm{an}} = I_{\mathrm{VH}} + (I_{\mathrm{VV}})_{\mathrm{an}} = \frac{7}{4}(I_{\mathrm{VV}})_{\mathrm{an}} = C\beta^2 \frac{k_{\mathrm{B}}T}{A + Lq^2}, \tag{4}$$

where β is the optical anisotropy measure of the aggregates, namely, the proportionality coefficient relating the dielectric anisotropy to the orientational order parameter, A is the first coefficient in the Landau–de Gennes expansion of the free energy in powers of the order parameter, L is the effective elastic constant of the spatial distortions of orientational order, $q = (4\pi n/\lambda)\sin(\theta/2)$, θ is the scattering angle, λ is the wavelength of light in vacuum, n is the refractive index, k_{B} is the Boltzmann constant, and C is an instrumental constant.

Figure 3 shows that $(I_{\mathrm{VV}})_{\mathrm{an}}^{-1}$ is indeed a linear function of q^2. By linear extrapolation to the limit of zero-angle scattering, we introduce the quantity

$$(I_0)_{\mathrm{an}}^{-1} = \Gamma_{\mathrm{an}}^{-1}(q = 0) = \frac{A}{C\beta^2 k_B T} = \frac{1}{C\beta^2 \chi}, \tag{5}$$
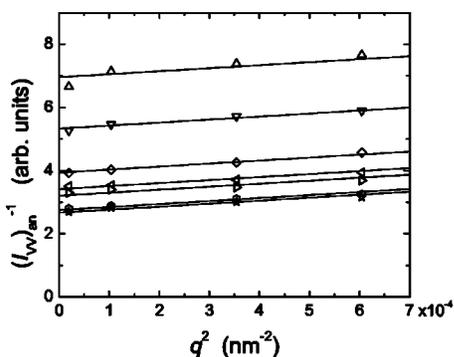
where

FIG. 3. Ornstein-Zernike plots for the anisotropic part of the polarized light scattered in the aqueous solution of DSCG. The solid lines represent a fit to Eq. (4).

$$\chi = \frac{k_B T}{A} \qquad (6)$$

is known as the susceptibility to the fluctuations of anisotropy [32,33]. Generally, in the vicinity of a weakly first-order transition

$$\chi = \Gamma_0 \varepsilon^{-\gamma}, \qquad (7)$$

where

$$\varepsilon = \frac{(T - T^*)}{T},$$

Γ_0 is the susceptibility amplitude, γ is the susceptibility exponent, and T^* is the temperature of the absolute stability of the isotropic phase. In the mean-field approximation [32,33] $\gamma = 1$ and

$$A = a(T - T^*), \qquad (8)$$

where $a = k_B / \Gamma_0$. The linear temperature dependence of A is well documented in the broad temperature range around the isotropic-to-nematic transition in thermotropic liquid crystals. Some deviations have been observed only in the close proximity of the transition [35,36,40–42] and were later explained by a coupling between orientational (nematic) and translational (smectic) fluctuations [35,36,39].

The case of the isotropic-to-nematic transition in aqueous solution of DSCG is very different. The experiment (Fig. 4) shows that the temperature dependence of $(I_0)_{an}^{-1}$ is strongly nonlinear. This nonlinearity increases with increase of temperature and exhibits a concave shape, opposite to the convexity observed in thermotropic nematics very close to the transition temperature. The factor T in the denominator of Eq. (7) does not play a significant role as in our experimental domain the temperature T differs from T^* less than by 3%. This nonlinear dependence might be interpreted in two different ways. The first possibility would be that Eq. (8) rewrites as $A = a(T - T^*)^\gamma$, where $\gamma > 1$. However, the temperature dependence of $(I_0)_{an}^{-1}$ remains reasonably linear near the transition point and our data do not fit this modified expression for A with a constant exponent $\gamma > 1$.

The second possibility is related to a peculiar nature of building blocks of the N phase, the rod-like aggregates. The
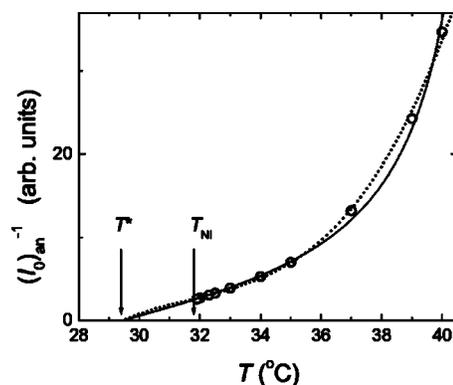

FIG. 4. Inverse intensity of the anisotropic light scattering in the aqueous solution of DSCG extrapolated to zero scattering angle. The symbols indicate experimental data. The solid curve represents a fit to Eq. (11). The dashed curve is a fit to Eq. (9).

aggregation number in these units should behave very differently from the aggregation number in many micelle-based surfactant solutions where it is restricted by the closed geometry of micelles. A possibility that the aggregate length, l, increases as the temperature decreases is suggested by sharp increase of the shear viscosity when the temperature is reduced, shown in Fig. 5. The change in the aggregate length $l = l(T)$ implies that the temperature stability limit of the isotropic phase, T^*, is no longer a temperature-independent constant. We thus modify the classic temperature dependence of A by including nonlinear terms and writing $A(T)$ in the form

$$A = a[T - T^*(T)],$$

$$T^* = T_0^* - \alpha_1(T - T_0^*) - \alpha_2(T - T_0^*)^2 - \alpha_3(T - T_0^*)^3, \qquad (9)$$

where a, $\alpha_{1,2,3}$, and T_0^* are constants. It is natural to expect that each value of the rod length $l = l(T)$ has its own value of $T^* = T^*(T)$ which would have been the temperature of the absolute stability of the isotropic phase if the rod length were "frozen." Obviously, the corresponding value of T^* will be high when l is large, while $T^* \to 0$ when l becomes very
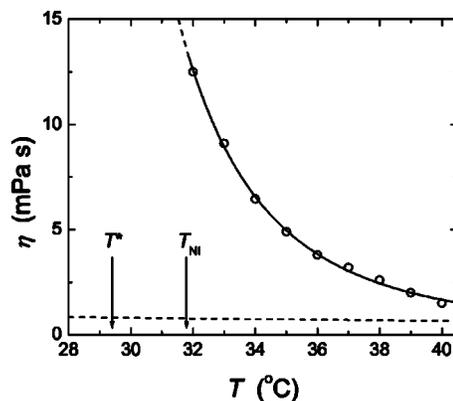

FIG. 5. Shear viscosity of the aqueous solution of DSCG. The solid curve represents a fit to Eq. (17). The dashed line represents the viscosity of water.
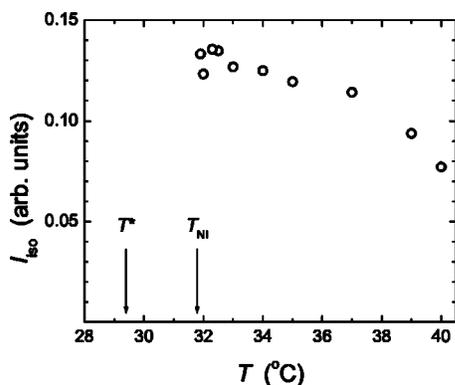
FIG. 6. Isotropic part (due to concentration fluctuations) of the light-scattering intensities in the aqueous solution of DSCG.
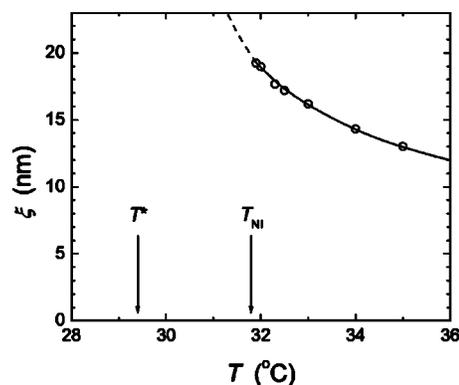

FIG. 7. Correlation length of the orientational fluctuations in the aqueous solution of DSCG. The solid curve represents values calculated with Eq. (13).

small as the nematic phase does not form at all. The linear coefficient α_1 does not change the temperature behavior of A, as it only renormalizes the coefficient a, i.e., $a \rightarrow a(1 + \alpha_1)$. Therefore, in the first (linear) approximation the effect of the elongation of the rods on T^* is absorbed by the coefficient a, which in turn cannot be separated from other prefactors in Eq. (5) and thus cannot be independently evaluated. Adopting $a/C\beta^2 = 1$, one can then use α_1, α_2, and α_3 as adjustable parameters. Equation (9) fits the experimental data presented in Fig. 4 reasonably well with the following parameters: $T_0^* = 302.65$ K (29.4 °C), $\alpha_1 = 0.566$, $\alpha_2 = -0.294$ K^{-1}, and $\alpha_3 = 0.042$ K^{-2}.

The aggregate elongation might lead to some increase of the optical anisotropy measure of the aggregates, β. Such a possibility is also in qualitative agreement with the experimental data. If one attributes the entire effect of nonlinearity in the temperature dependence of $(I_0)_{an}^{-1}$ to the change in β, this parameter can be empirically represented as

$$\beta = \beta^* (1 - b\varepsilon^2)^{1/2}, \tag{10}$$

where β^* is the value of β at $T = T^*$, with $b = 582$. Therefore, the temperature dependence of the zero-angle intensity can be approximated by

$$(I_0)_{an} = C(\beta^*)^2 (1 - b\varepsilon^2)(a\varepsilon)^{-1}. \tag{11}$$

The intercept of the extrapolated inverse intensity with the temperature axis yields $T^* = 29.4$ °C (Fig. 4), which is about 2.4 °C lower than $T_{NI} = 31.8$ °C and which is equal to the value of T_0^* obtained with Eq. (9).

It is difficult to separate unambiguously the non-linear effects implied by Eq. (9) and by Eq. (10), as qualitatively both mechanisms lead to the same unusual concave character of the temperature dependence of $(I_0)_{an}^{-1}$. Finally, note that the elastic constant L is assumed to be temperature independent and possible increase in β caused by the elongation of rods could be compensated by the decrease in the number of rods (as the total number of the DSCG molecules available for the construction of aggregates is constant).

Note that the concentration fluctuations also play some role near the transition temperature T_{NI} since I_{iso} increases on cooling, Fig. 6. However, the intensity of the isotropic light-scattering does not diverge at $T = T^*$.

We rewrite Eq. (4) in the form accessible for the estimation of the correlation length $\xi = \sqrt{L/A}$ [32]:

$$I_{an} = C\beta^2 \frac{\chi}{1 + \xi^2 q^2}, \tag{12}$$

so that in the vicinity of the phase transition, where we can still use the approximation $A \simeq a(T - T^*)$ and $\varepsilon \simeq (T - T^*)/T^*$, one has

$$\xi = \xi_0 \varepsilon^{-1/2}, \tag{13}$$

where

$$\xi_0 = \sqrt{\frac{L}{aT^*}} \tag{14}$$

is an amplitude of the correlation length. The correlation length as a function of temperature is shown in Fig. 7. From these data and Eq. (13) we obtain $\xi_0 = 2$ nm. This value appears to be close to the larger dimension of the DSCG molecule and to the diameter of aggregates [7,43]. For comparison, in the thermotropic liquid crystal MBBA, $\xi_0 \simeq 0.6$ nm [40,41], which is close to the width of the MBBA molecule.

IV. DYNAMICS OF PRETRANSITIONAL FLUCTUATIONS

The orientational and translational dynamics of anisotropic scatterers is often complicated as it may be represented by several different modes [37–39,44,45]. Therefore, the correlation function may generally consists of several exponentials. This is why it is difficult to extract the decay times by direct approximation of the correlation function to multi-exponentials. Therefore, we have analyzed the distributions of decay times, which were obtained from the correlation functions with the regularization method [46,47]. From these distributions we obtained the positions of most pronounced dynamic modes.

Figure 8 shows the distribution of the decay times of dynamic correlation function in the isotropic phase of the DSCG solution for $\theta = 19°$ and VV polarization. The distribution is shown as the projection of a three-dimensional plot
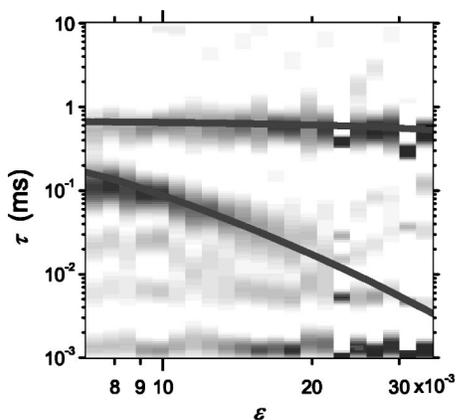
FIG. 8. Projection of the distributions of the decay time of the dynamic correlation function in the aqueous solution of DSCG at $\theta=19°$ and different $\varepsilon=(T-T^*)/T$. Two relaxation modes (shown as thick solid curves) have been calculated with Eq. (19) ("fast" mode, orientational fluctuations) and with Eq. (19) ("slow" mode, diffusion of concentration fluctuations).

in which the distribution values are normalized by their integrals [48]. For each temperature one can clearly distinguish two major characteristic modes. One mode is rapidly slowing down when the temperature approaches the isotropic-nematic transition temperature T_{NI} and the other one is almost independent on temperature. We analyzed the q-dependence of these modes (Fig. 9 shows an example for $\varepsilon=10^{-2}$) and found that the slowing-down mode only slightly depends on q, while the other mode strongly depends on q (approximately as q^2). This q^2-dependent mode appears in the VV polarization and is not seen in the VH component. We conclude that the q^2-dependent mode is a diffusion mode of the concentration fluctuations, while the slowing-down mode is associated with the relaxation of the orientational fluctuations.

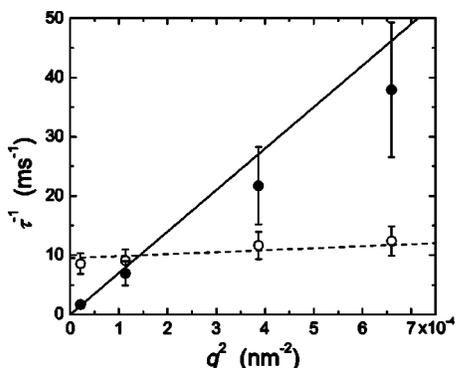The q-dependent diffusion relaxation time can be written as

FIG. 9. Wave-number dependence of the two relaxation modes in the aqueous solution of DSCG at $\varepsilon=(T-T^*)/T=10^{-2}$. The open circles indicate orientational relaxation times and the solid circles indicate translational diffusion times. The slope of the solid line is the translational diffusion coefficient. The dashed line is calculated with Eq. (18).

$$\tau_D = \frac{1}{Dq^2}, \tag{15}$$

where D is the translational diffusion coefficient that can be obtained from the slopes of τ_D^{-1} vs q^2. The linear fit shown in Fig. 9 yields $D=7\times10^{-11}$ m^2/s. If we assume that the concentration fluctuations are caused mostly by diffusion of the rods, the diffusion coefficient can be roughly related to the rods' length l and diameter d, being some average over the diffusion constants parallel and perpendicular to the rod axis [49]:

$$D = \frac{k_B T}{3\pi\eta_s l} \ln \frac{l}{d}, \tag{16}$$

where η_s is the characteristic medium viscosity. The fact that the translational diffusion coefficient is almost temperature independent (see Fig. 8) suggests that η_s in Eq. (16) depends on temperature weakly. This is why, we associate η_s with the viscosity of solvent (water), while the actual viscosity of solution exhibits a steep temperature dependence, shown in Fig. 5. With $\eta_s\simeq0.7$ mPa s, $D=7\times10^{-11}$ m^2/s and $d\simeq2$ nm, one estimates $l\simeq20$ nm. This value is most probably an overestimate as in Eq. (16) we used the viscosity of the pure solvent.

The actual shear viscosity data were approximated by the Vogel-Fulcher equation:

$$\eta = \eta_0 \exp\left(\frac{B}{T-T_0}\right) \tag{17}$$

with the fitting parameters $\eta_0=0.0136$ mPa s, $B=130$ K, and $T_0=286$ K, which is the temperature of the apparent divergence of viscosity. The Vogel-Fulcher equation is a generalization of the standard Arrhenius equation (in which $T_0=0$) and is applied for the liquids exhibiting a glass transition [50]. A glass-like character of molecular ordering was also found in solutions of disk-like lyomesogens [51].

As compared with the viscosity of the solvent (water), the viscosity of the DSCG aqueous solution demonstrates an anomalous growth upon approaching the transition temperature T_{NI}. Such an anomaly does not usually exist in the isotropic phase of thermotropic nematics and, most plausibly, can be attributed to the elongation of supramolecular aggregates (rods) of DSCG molecules when the temperature decreases.

In contrast to the diffusion mode, the orientational relaxation mode strongly depends on the distance to the isotropic-nematic phase transition. As in the case of pretransitional slowing down in the isotropic phase of thermotropic nematics, the relaxation time of a non-conserved order parameter generally is proportional to the product of the friction coefficient (viscosity) and q-dependent susceptibility [32,33]:

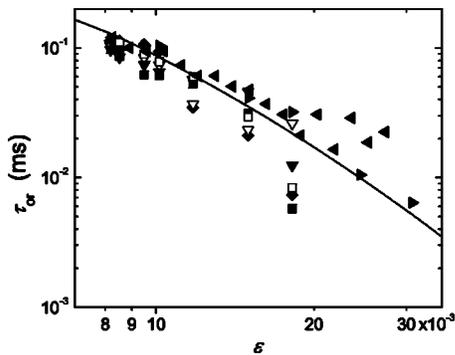$$\frac{1}{\tau_{or}(q)} = \frac{A+Lq^2}{\eta}. \tag{18}$$

FIG. 10. Orientational relaxation times (in the $q=0$ limit) in the aqueous solution of DSCG obtained for different scattering angles and different polarizations as a function of $\varepsilon=(T-T^*)/T$. Open symbols correspond to VH, solid symbols to VV: ■—135°, VV, □—135°, VH, ▼—90°, VV, ▽—90°, VH, ◆—45°, VV, ▶—19°, VV, ◀;—19°, VV (second run). The solid curve was calculated with Eqs. (19) and (20) with $l_0=7$ nm.

Note the difference with the diffusion relaxation time defined by Eq. (19): the orientational relaxation time only weakly depend on q unless $A=a(T-T^*)$ is zero. This is characteristic for the dynamics of a nonconserved order parameter.

Thus, the temperature dependence of the orientational mode can be described by the critical growth of the susceptibility and, in addition, by the anomalous growth of the shear viscosity η. In the $q=0$ limit

$$\tau_{\mathrm{or}}=\tau_{\mathrm{or}}(q=0)=\frac{\eta}{A}\simeq\frac{\tau_0\eta}{\eta_s\varepsilon} \qquad (19)$$

with τ_0 being a characteristic microscopic orientational relaxation time. In spite of considerable scattering in the data obtained for different angles and different polarizations (Fig. 9), Eq. (19) gives a remarkably good prediction and essentially grasps the physics of the pretransitional dynamics. In Fig. 10 we show the dependence of $\tau_{\mathrm{or}}(\varepsilon)$ calculated from Eq. (19) with the primary time-scale amplitude τ_0 being represented in the form

$$\tau_0=\frac{l_0^3\eta_s}{k_{\mathrm{B}}T}. \qquad (20)$$

At the transition temperature, $T_{\mathrm{NI}}=31.8$ °C, $\tau_0\simeq50$ ns with the length-scale amplitude $l_0\simeq7$ nm. Note the inverse-susceptibility coefficient $a=A/(T-T^*)$, of the order of $k_{\mathrm{B}}/l_0^3\simeq40$ J/m³K [33]), is absorbed in the definition of τ_0.

A relation between the amplitude l_0 and the actual size of DSCG rod-like aggregates depends on a particular model that is yet to be developed for aqueous DSCG solutions. If one assumes that $l_0\simeq7$ nm is close to the length l of the primary aggregates and that the anomaly in the shear viscosity is caused by the elongation of rods, one can estimate the length of rods as

$$l=l_0\left(\frac{\eta}{\eta_s}\right)^{1/3}. \qquad (21)$$

As the ratio η/η_s increases from 2.5 at 40 °C to 16.9 at 32 °C, the length l increases from 9 nm to 17 nm, respectively. It is interesting that this length appears to be of the same order as an *a priori* estimate of 20 nm. Such an estimate seems reasonable as it is within the order of the correlation length ξ, which increases from 10 to 20 nm in the same temperature interval. Taking into account that the intermolecular distance along the aggregate axis is $\delta=0.34$ nm [1,2,7], we conclude that the aggregate length changes in the range $l=(25-50)\delta$ in the temperature range 39–32 °C. Interesting questions yet to be answered are whether the aggregation of DSCG molecules is coupled with fluctuations of the nematic order parameter and whether the diffusion dynamic mode is coupled with the orientational dynamic mode.

The term "chromonics" covers systems with very different types of aggregates. A common property, which all chromonics share, is a stacking of the molecules forming aggregates, but the structure of the aggregates can be very different. Moreover, not all such systems are necessarily forming mesophases. Collings *et al.* [52] have deduced from a resonant light-scattering experiment that in the case of different apparently nonmesomorphic chromonic molecules (porphirin) the aggregates are about 0.8 μm long and 0.04 μm thick, which corresponds to about 20 molecules across the diameter of the aggregate. The length-thickness ratio of these rods is about 20, which is not much different from the ratio $l/d\sim10$ that we estimate for the DSCG aggregates above the NI transition.

V. CONCLUSIONS

Our results show that the main features of the pretransitional fluctuations in the isotropic phase of lyotropic chromonic liquid crystal of DSCG are similar to the phenomena observed in thermotropic liquid crystals. These features include the following.

(1) A growth of the orientational susceptibility and correlation length of the pretransitional fluctuations of anisotropy, qualitatively in accordance with the Landau–de Gennes theory.

(2) A critical slowing-down: the relaxation time of the orientational (order parameter) fluctuations diverges at the stability limit of the isotropic phase, being proportional to the solution viscosity and orientational susceptibility.

However, there are some features that make the pretransitional phenomena in the lyotropic chromonic liquid crystal DSCG even more interesting.

(1) There is a significant contribution to the light-scattering intensity from concentration fluctuations (10% near the transition point T_{NI} and 60% at $T=T_{\mathrm{NI}}+8$ °C).

(2) There is a significant deviation in the temperature behavior of the inverse intensity from the linear (Curie-Weiss) law possibly caused by the temperature dependence of the aggregate's length. This temperature dependence may result in the nonlinear temperature dependence of the Landau–de Gennes coefficient A, Eq. (8) and effective optical anisotropy, Eq. (10).

(3) The shear viscosity exhibits an anomalous growth with decrease of temperature, being associated with the elongation of the supramolecular aggregates.

Our current description of the pretransitional phenomena in aqueous solutions of DSCG is intended to grasp only the most essential physical features. Further experimental studies of an expected coupling between the orientational and translational dynamic modes, as well as a coupling between the nematic order parameter and supramolecular aggregation in LCLC, are highly desirable. Finally, one should also bear in mind that the length of aggregates in LCLC might also be a function of the sample prehistory associated with flows, temperature regimes, etc. In the present work, we took the measures to reduce the effect by heating all the samples to 55 °C prior the data acquisition, but the subject itself is worth separate studies.

[1] J. E. Lydon, in *Handbook of Liquid Crystals*, edited by D. Demus, J. Goodby, G. W. Gray, H.-W. Spiess, and V. Vill (Wiley-VCH, New York, 1998), Vol. 2B, Chap. XVIII, p. 981.

[2] J. Lydon, Curr. Opin. Colloid Interface Sci. **3**, 458 (1998); **8**, 480 (2004).

[3] A. S. Vasilevskaya, E. V. Generalova, and A. S. Sonin, Russ. Chem. Rev. **58**, 904 (1989).

[4] T. K. Attwood and J. E. Lydon, Mol. Cryst. Liq. Cryst. **108**, 349 (1984).

[5] M. Kleman and O. D. Lavrentovich, *Soft Matter Physics: An Introduction* (Springer, New York, 2003).

[6] J. V. Champion and G. H. Meeten, J. Pharm. Sci. **62**, 1589 (1973).

[7] N. H. Hartshorne and G. D. Woodard, Mol. Cryst. Liq. Cryst. **23**, 343 (1973).

[8] J. E. Lydon, Mol. Cryst. Liq. Cryst. Lett. **64**, 19 (1980); see also N. H. Hartshorne and G. D. Woodard, *ibid.* **64**, 153 (1980).

[9] L. J. Yu and A. Saupe, Mol. Cryst. Liq. Cryst. **80**, 129 (1982).

[10] H. Lee and M. M. Labes, Mol. Cryst. Liq. Cryst. **84**, 137 (1982).

[11] D. Goldfarb, M. M. Labes, Z. Luz, and R. Poupko, Mol. Cryst. Liq. Cryst. **87**, 259 (1982).

[12] H. Lee and M. M. Labes, Mol. Cryst. Liq. Cryst. **91**, 53 (1983).

[13] D. Perahia, D. Goldfarb, and Z. Luz, Mol. Cryst. Liq. Cryst. **108**, 107 (1984).

[14] D. Goldfarb, Z. Luz, N. Spielberg, and H. Zimmermann, Mol. Cryst. Liq. Cryst. **126**, 225 (1985).

[15] G. J. T. Tiddy, D. L. Mateer, A. P. Ormerod, W.J. Harrison, and D. J. Erdwards, Langmuir **11**, 390 (1995).

[16] P. Camorani, M. Furier, O. Kachkovskii, Yu. Piryatinsky, Yu. Slominskii, and V. Nazarenko, Semicond. Phys., Quantum Electron. Optoelectron. **4**, 229 (2001).

[17] Y. W. Hui and M. M. Labes, J. Phys. Chem. **90**, 4064 (1986); V. Ramesh, H.-S. Chien, and M. M. Labes, *ibid.* **91**, 5937 (1987).

[18] J. F. Dreyer, US Patent 2,544,659 (March 13, 1951).

[19] T. Sergan, T. Schneider, J. Kelly, and O. D. Lavrentovich, Liq. Cryst. **27**, 567 (2000).

[20] Y. Bobrov, C. Cobb, P. Lazarev, P. Bos, D. Bryant, and H. Wonderly, SID, Int. Symp. of Technical Papers, Long Beach, CA, 31 1102 (2000).

[21] S. Remizov, A. Krivoshchepov, V. Nazarov, and A. Grodsky, Mol. Mater. **14**, 179 (2001).

[22] W. C. Yip, H. S. Kwok, V. M. Kozenkov, and V. G. Chigrinov, Displays **22**, 27 (2001).

[23] D. Matsunaga, T. Tamaki, H. Akiyama, and K. Ichimura, Adv. Mater. (Weinheim, Ger.) **14**, 1477 (2002).

[24] S. W. Tam-Chang, W. Seo, I. K. Iverson, and S. M. Casey, Angew. Chem., Int. Ed. **42**, 897 (2003).

[25] C. Ruslim, M. Hashimito, D. Matsunaga, T. Tamaki, and K. Ichimura, Langmuir **20**, 95 (2004).

[26] S. W. Tam-Chang, I. K. Iverson, and J. Helbley, Langmuir **20**, 342 (2004).

[27] T. Sergan and J. Kelly, Liq. Cryst. **27**, 1481 (2000).

[28] M. Lavrentovich, T. Sergan, and J. Kelly, Liq. Cryst. **30**, 851 (2003).

[29] T. Schneider and O. D. Lavrentovich, Langmuir **16**, 5227 (2000); T. Schneider, K. Artyushkova, J. E. Fulghum, L. Broadwater, A. Smith, and O. D. Lavrentovich (unpublished).

[30] J. Jacob, M. A. Anisimov, J. V. Sengers, V. Dechabo, I. K. Yudin, and R. W. Gammon, Appl. Opt. **40**, 4160 (2001).

[31] I. L. Fabelinskii, *Molecular Scattering of Light* (Plenum, New York, 1968).

[32] P. G. de Gennes and J. Prost, *The Physics of Liquid Crystals* (Clarenton, Oxford, 1993).

[33] M. A. Anisimov, *Critical Phenomena in Liquids and Liquid Crystals* (Gordon and Breach, Philadelphia, 1991).

[34] E. M. Lifshitz and L. P. Pitaevskii, *Physical Kinetics* (Oxford, New York, 1993).

[35] A. Gohin, C. Destrade, H. Gasparoux, and J. Prost, J. Phys. (France) **44**, 427 (1983).

[36] M. A. Anisimov, V. I. Labko, G. L. Nikolaenko, and I. K. Yudin, Mol. Cryst. Liq. Cryst., Lett. Sect. **2**, 77 (1985); JETP Lett. **45**, 111 (1987); Mol. Cryst. Liq. Cryst. **146**, 421 (1987).

[37] B. J. Berne and R. Pecora, *Dynamic Light Scattering with Applications to Chemistry, Biology, and Physics* (Wiley, New

York, 1976).

[38] K. Zero and R. Pecora, in *Dynamic Light Scattering. Applications of Photon Correlation Spectroscopy*, edited by R. Pecora (Plenum, New York, 1985), p. 59.

[39] A. Yu. Val'kov, V. P. Romanov, and A. N. Shalaginov, Phys. Usp. **37**, 139 (1994).

[40] T. W. Stinson and J. D. Litster, Phys. Rev. Lett. **25**, 503 (1970); **30**, 688 (1973).

[41] E. Gulary and B. Chu, J. Chem. Phys. **62**, 798 (1975).

[42] L. V. Adjemyan, L. T. Adjemyan, A. Yu. Val'kov, L. A. Zubkov, I. A. Mel'nik, and V. P. Romanov, Sov. Phys. JETP **60**, 712 (1984).

[43] Yu. A. Nastishin, H. Liu, T. Schneider, V. Nazarenko, R. Vasyuta, S. V. Shiyanovskii, and O. D. Lavrentovich (in preparation).

[44] M. Doi and S. F. Edwards, *The Theory of Polymer Dynamics* (Clarenton, Oxford, 1992).

[45] P. S. Russo, in *Dynamic Light Scattering. The Method and Some Applications*, edited by W. Brown (Clarendon, Oxford,

1993).

[46] E. R. Pike, in *Pharmaceutical Emulsions and Suspensions. Drugs and the Pharmaceutical Sciences*, edited by F. Nielloud and G. Marti-Mestres (Dekker, New York, 2000), Vol. 105, p. 609.

[47] S. W. Provencher, Comput. Phys. Commun. **27**, 213 (1982).

[48] A. F. Kostko, M. A. Anisimov, and J. V. Sengers, Phys. Rev. E **66**, 020803(R) (2002).

[49] J. Riseman and J. G. J. Kirkwood, Chem. Phys. **18**, 512 (1950).

[50] R. G. Larson, *The Structure and Rheology of Complex Fluids* (Oxford University Press, Oxford, 1999).

[51] I. Drevenšek Olenik, L. Spindler, M. Čopič, H. Sawade, D. Krüerke, and G. Heppke, Phys. Rev. E **65**, 011705 (2002).

[52] P. J. Collings, E. J. Gibbs, T. E. Starr, O. Vafek, C. Yee, L. A. Pomerance, and R. F. Pasternack, J. Phys. Chem. B **103**, 8474 (1999).